Field-based decadal wave attenuating capacity of combined tidal flats and salt marshes

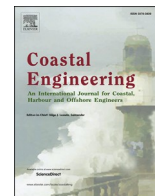Willemsen, Pim W.J.M.; Borsje, Bas W.; Vuik, Vincent; Bouma, Tjeerd J.; Hulscher, Suzanne J.M.H.

Important note
To cite this publication, please use the final published version (if applicable).
Please check the document version above.

Field-based decadal wave attenuating capacity of combined tidal flats and salt marshes

Pim W.J.M. Willemsen [a,b,c,*], Bas W. Borsje [a], Vincent Vuik [d,e], Tjeerd J. Bouma [b], Suzanne J.M. H. Hulscher [a]

[a] *University of Twente, Water Engineering & Management, P.O. Box 217, 7500 AE, Enschede, the Netherlands*
[b] *NIOZ Royal Netherlands Institute for Sea Research and Utrecht University, Department of Estuarine and Delta Systems, P.O. Box 140, 4400 AC, Yerseke, the Netherlands*
[c] *Deltares, Department of Ecosystems and Sediment Dynamics, P.O. Box 177, 2600 MH, Delft, the Netherlands*
[d] *Delft University of Technology, Faculty of Civil Engineering and Geosciences, P.O. Box 5048, 2600 GA, Delft, the Netherlands*
[e] *HKV Consultants, P.O. Box 2120, 8203 AC, Lelystad, the Netherlands*

ARTICLE INFO

ABSTRACT

Foreshores consisting of both bare tidal flats and vegetated salt marshes are found worldwide and they are well studied for their wave attenuating capacity. However, most studies only focus on the small scale: just some isolated locations in space and only up to several years in time. In order to stimulate the implementation of foreshores serving as reliable coastal defense on a large scale, we need to quantify the decadal wave attenuating capacity of the foreshore on the scale of an estuary. To study this, a unique bathymetrical dataset is analyzed, covering the geometry of the Westerschelde estuary (The Netherlands) over a time-span of 65 years. From this dataset, six study sites were extracted (both sheltered sites and exposed sites to the prevailing wind direction) and divided into transects. This resulted in 36 transects covering the entire foreshore (composed of the bare tidal flat and the vegetated salt marsh). The wave attenuation of all transects under daily conditions (with and without vegetation) and design conditions (i.e. events statistically occurring once every 10,000 years) was modelled.

Overall, the spatial variability of the geometry of a single foreshore was observed to be much larger than the temporal variability. Temporal changes in salt marsh width did not follow the variability of the entire foreshore. Both under daily and design conditions, vegetation contributes to decreasing wave energy and decreases the variability of incoming wave energy, thereby decreasing the wave load on the dike. The southern foreshores, sheltered from the prevailing wind direction, were more efficient in wave attenuation than the exposed northern foreshores. A linear relation between marsh width and wave attenuation over a period of 65 years was observed at all marshes. The present study provides insights needed to calculate the length of a salt marsh to obtain a desired minimum wave attenuating capacity.

1. Introduction

Estuaries are complex landscapes shaped by bio-physical interactions and anthropogenic influences. They are located at the interface of fresh riverine and saline coastal waters, providing a range of ecosystem services such as habitat provision, food production, space for recreation and accessibility over water (e.g. Barbier et al., 2010). However, living near estuaries also comes with flood risks from riverine and coastal sources. Nevertheless, the population density in these areas is high and still growing (Small and Nicholls, 2003; Syvitski et al., 2009). Moreover, extreme storm events and sea level rise increase flood risks in the coastal zone, as an insurmountable consequence of climate change (Donnelly et al., 2004; Knutson et al., 2010; Lin et al., 2012; IPCC, 2014). As a result, estuaries become increasingly vulnerable to flooding and communities inhabiting these areas are in need of improved flood protection.

The population and economic value of the estuaries hinterland are generally protected by conventional coastal engineering solutions, such as groins, revetments, breakwaters and sea walls. Those conventional measures are increasingly challenged by regional and global changes, including climate change-induced Sea Level Rise (SLR), increased storm intensity and land subsidence (Syvitski et al., 2009). These conventional

solutions are static and do not adapt to a changing climate (Borsje et al., 2011; Temmerman et al., 2013).

Foreshores, consisting of a bare tidal flat and vegetated salt marsh, can serve as add-on to conventional coastal defenses (Kirwan et al., 2010; Gedan et al., 2011; Moller et al., 2014). Firstly, salt marshes occur widely in tempered climate zones (Mcowen et al., 2017), so they can be applied globally. Secondly, foreshores can dissipate wave energy due to the bottom profile and vegetation (e.g. Vuik et al., 2016), consequently being suitable to attenuate wave energy in front of a dike. Thirdly, marshes are sustainable and in that they can cope, to a certain extent, with SLR (Kirwan and Megonigal, 2013; Kirwan et al., 2016). By dissipating hydrodynamic energy, sediment is trapped in the marsh, enabling vertical growth of the bed (Bouma et al., 2007; Van Wesenbeeck et al., 2008).

Thus, salt marshes have high potential for a contribution to coastal protection, despite the uncertainty as a consequence of using vegetation and thereby introducing intrinsic biological factors (Bouma et al., 2014). Moreover, salt marshes and tidal flats might be cost-effective locally and more flexible and thereby suitable for adaptive coastal management compared to conventional coastal engineering solutions (Turner et al., 2007; Broekx et al., 2011; Cheong et al., 2013), which is a prerequisite for dealing with flood risks due to climate change (Gersonius et al., 2013).

So far, the significant wave attenuating capacity of foreshores within the time scale of events (e.g. extreme storm events) is proven for specific aspects in wave flumes (e.g. Coops et al., 1996), and give mechanical understanding of vegetation stiffness (Bouma et al., 2005), standing biomass, (Bouma et al., 2010), extreme storms (Moller et al., 2014) and wave-current interaction (Maza et al., 2015). Field studies give insights in wave attenuation with realistic conditions on a larger scale (Möller, 2006; Yang et al., 2012; Vuik et al., 2016). These studies prove the significant wave attenuating capacity for a specific setting of a foreshore for a specific moment in time: a snapshot. Within the timescale of seasons, field measurements at transects perpendicular to the marsh edge between salt marsh and tidal flat suggest a relative stable salt marsh with a more variable seaward situated tidal flat (Andersen et al., 2006; Vuik et al., 2018a; Willemsen et al., 2018). Moreover, at this seasonal timescale, measurements over a stretch of salt marsh (50 m width), suggest a continuous contribution of the marsh to wave attenuation (Vuik et al., 2018a).

Although all these studies actually measure the wave attenuation, they still focus on the relative small scale, i.e. some isolated locations in space and at most up to several years in time, and they do not capture extreme conditions over long-term salt marsh settings. Moreover, to our knowledge superimposing extreme conditions over long-term foreshore settings measured in the field, to give unique long-term insights, has not been done before. The long-term persistence of wave-attenuating ecosystems has been identified as a key-bottle neck hampering application of intertidal habitats for coastal protection (Bouma et al., 2014). Moreover, wave attenuation is known to be highly location-specific, depending on bio-physical settings such as foreshore width and the geometry of both the vegetated salt marsh and bare tidal flat (Vuik et al., 2016). Hence, the key question addressed in this paper is: what is the variability of foreshores, consisting of salt marshes and adjacent tidal flats, in an estuary over a decadal time-scale; and to what extent can foreshores safely act as additional defense measure? We will quantify the long-term (50+ years) variability of the wave attenuating capacity of foreshores in a full estuary, by combined long-term large-scale bathymetrical field data and numerical model analysis for calculating wave attenuation.

The structure of this paper is as follows. In Section 2 the study area is introduced, followed by a description of the long-term bathymetrical data. Consecutively the numerical model analysis for calculating wave attenuation is described, including vegetation representation and the scenarios that were assessed. Section 3 presents the variability of the bathymetry of the foreshore, followed by the contribution of the foreshore to wave attenuation under extreme scenarios and under daily scenarios, that have not been measured before. In section 4 the main findings of this paper are discussed. We end by drawing some conclusions in Section 5.

2. Bathymetrical field data analysis and wave modelling

2.1. Long-term foreshore elevation

Historical elevation data of foreshores, from the subtidal up to the higher elevated parts, which are only submerged during extreme high water, is scarce. In general, bathymetrical data representing the subtidal area has sufficient coverage. However, the data coverage for the higher elevated vegetated salt marsh is often lacking. In addition, long-term (50+ year) datasets with consecutively collected elevation data is even more scarce. Nevertheless, such datasets are available for the entire Westerschelde estuary in the Netherlands. In the Westerschelde estuary, multiple foreshores are present (Fig. 1), which can be differentiated by the prevailing wind direction being southwest. This results in a dichotomy of wind exposure, with foreshores at the northern shores being exposed and foreshores at the southern shores being sheltered from the prevailing wind direction (Callaghan et al., 2010). The long-term wave attenuating capacity of six foreshores, three at the exposed and three at the sheltered shores in the Westerschelde (Fig. 1), was analyzed. Elevation data for those nearshore areas were captured in extensive bathymetrical datasets, called 'Vaklodingen'. The data was collected since 1925–1935 by the Ministry of Infrastructure and the Environment (former Ministry of Transport Public Works and Water Management). After post-processing, the data is stored in grids with a cell size of 20 × 20 m (De Kruif, 2001; Wiegman et al., 2005). The vertical accuracy of the Vaklodingen data was 0.54 m in the 1950s increasing to 0.11 m since 2001 (Marijs and Parée, 2004).

We constructed two-dimensional transects, to enable assessment of the wave attenuating capacity (cf. Horstman et al., 2014). Bathymetrical data from the Vaklodingen was interpolated over the transects. The direction of the transects was parallel to the wave direction under design conditions (i.e. extreme event statistically occurring once every 10,000 years), obtained from a database with the results of 2D wave simulations, carried out in the context of dike safety assessments in the Netherlands (Gautier and Groeneweg, 2012; Groeneweg and Van Nieuwkoop, 2015). Transects that interfered with the land boundary, due to the position of the study site in the curvature of the dike, were excluded (i.e. the average design wave direction for a foreshore was just landward directed due to the shape of the foreshore). The alongshore spacing between transects (i.e. number of transects over a certain alongshore foreshore length) was selected in a way to capture the alongshore variability of the geometry and wave attenuation. This spacing was based on a transect refinement study (section 2.2.3). For determining the foreshore width, mean high water spring (MHWS) was used to represent the landward boundary. The seaward boundary of the foreshore was represented by mean low water spring (MLWS). Both water levels were assumed to be static over time, although an increase of the tidal amplitude over time has been observed in the Westerschelde (Taal et al., 2015), possibly changing the boundaries of the transects as a consequence. However, the hydrodynamic input parameters also change with a changing tidal amplitude, as it is assumed resulting in only minor changes to the wave attenuating capacity. Missing data causing incomplete transects at the intertidal or higher parts were interpolated over time per transect (cf. Vuik et al., 2019). In case the first year to be analyzed from a certain transect was incomplete, the known position of the dike toe was used for spatial interpolation, after which temporal interpolation was applied.

2.2. Modelling wave attenuation

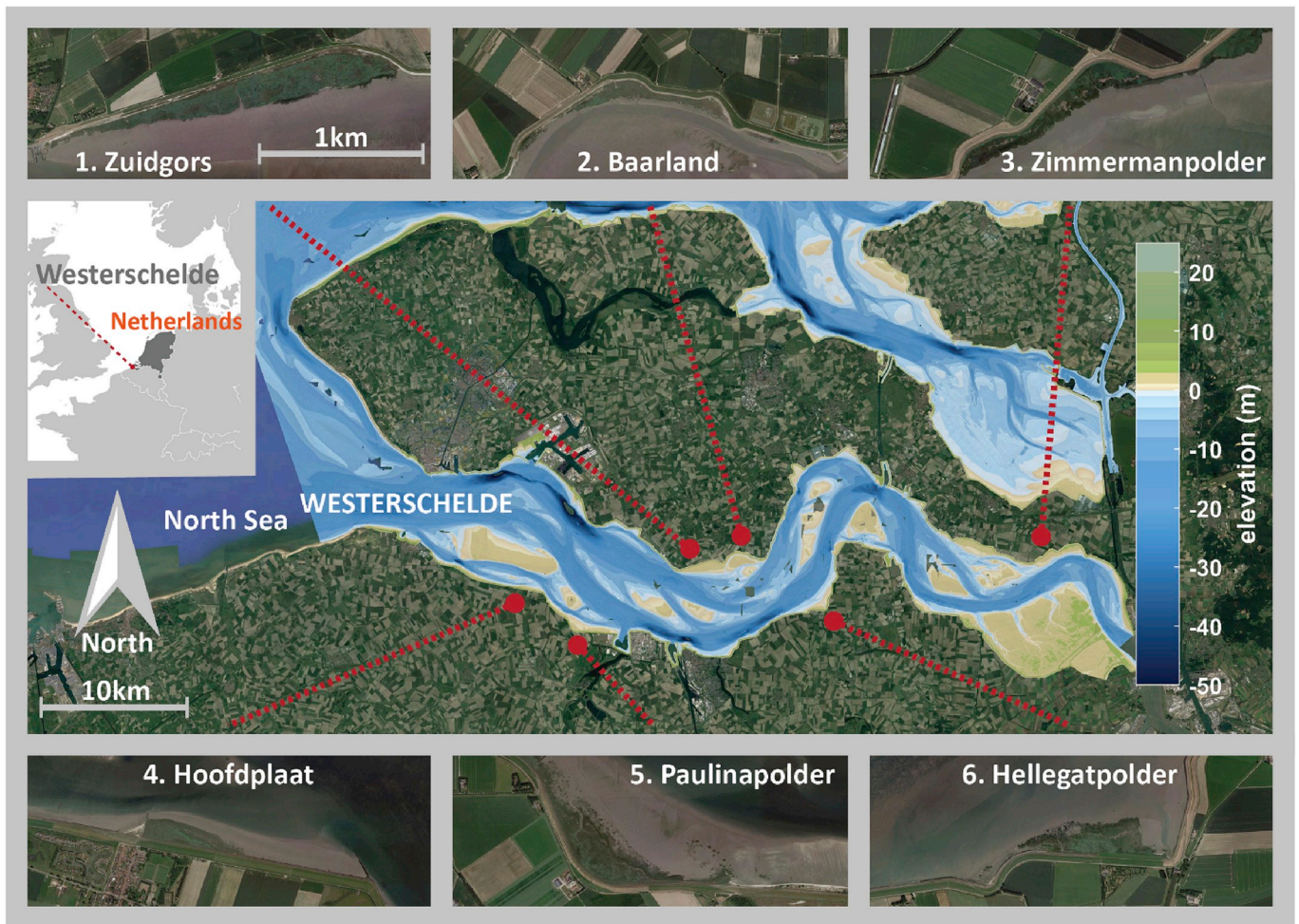Wave attenuation over the foreshore was computed using the

Fig. 1. Six analyzed foreshores (top and bottom panels) in the Westerschelde, indicated with red dots (center), located in the Southwestern part of the Netherlands (see inlay in center panel). Bathymetrical data of 2014 is presented in the center panel (elevation in meter with respect to mean sea level). (For interpretation of the references to color in this figure legend, the reader is referred to the Web version of this article.)

spectral wave model SWAN (Simulating WAves Nearshore; Booij et al., 1999; Ris et al., 1999). In this model, the vegetation module for wave attenuation was developed by Mendez and Losada (2004) and implemented in SWAN by Suzuki et al. (2012). The model was calibrated,

validated and applied previously on two foreshores in the southwestern delta of the Netherlands: 3. Zimmermanpolder (Bath) at the exposed northern shore and 6. Hellegatpolder at the sheltered southern shore (Fig. 1), where energy dissipation (i.e. wave heights) by foreshores
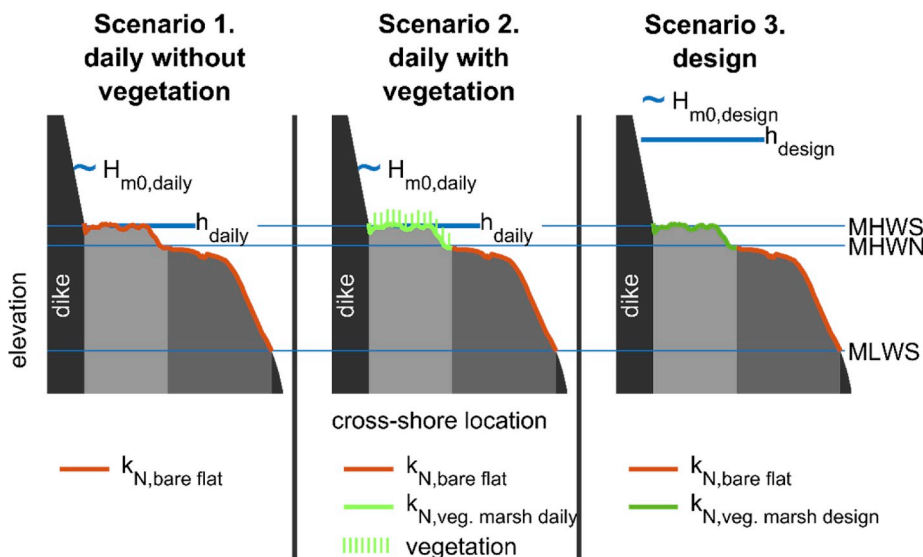
Fig. 2. Schematic overview of the foreshore, consisting of a bare tidal flat (dark grey), vegetated salt marsh (light grey) and dike (black) for obtaining wave attenuation under different scenarios. Hydrodynamic parameters used are: mean high water spring (MHWS), mean high water neap (MHWN), mean low water spring (MLWS), water level (h), significant wave height (H_{m0}) and the Nikuradse roughness length (k_N). Scenarios assessed were: (1) daily without explicitly accounting for vegetation by using a single Nikuradse roughness length $k_{N,bare\ flat}$, (2) daily with explicitly accounting for vegetation by using a different Nikuradse roughness length for the bare foreshore ($k_{N,\ bare\ flat}$) and the bed of the vegetated foreshore under the vegetation ($k_{N,\ veg.\ marsh\ daily}$) and explicitly taking into account vegetation structures, (3) design conditions by using a different Nikuradse roughness length for the bare foreshore ($k_{N,\ bare\ flat}$) and for the vegetated foreshore ($k_{N,\ veg.\ marsh\ design}$) by taking into account stem breakage and hydrodynamic parameters under design conditions.

Table 1
Characteristics of the analyzed foreshores and input values for wave modelling.

Study site	Local water level boundaries			Vaklodingen data		Local design conditions			
	MLWS (m)	MHWN/ marsh edge (m)	MHWS/Daily water level (m)	Period of data availability (year - year)	Number of years included (−)	Design water level (m)	Design wave height (m)	Design wave period (s)	Design wave direction (°)
	h_{MLWS}	h_{MHWN}	h_{daily}	–	–	h_{norm}	$H_{m0,design}$	$T_{m-1,0,design}$	dir
1. Zuidgors	−2.31	1.85	2.63	1955–2015	37	6.04	1.655	4.725	233
2. Baarland	−2.28	1.83	2.62	1955–2015	37	6.13	1.72	4.35	238
3. Zimmerman-polder	−2.46	2.14	3.04	1951–2015	51	6.71	1.82	4.15	212
4. Hoofdplaat	−2.06	1.59	2.34	1950–2015	42	5.78	2.36	4.55	323
5. Paulina	−2.16	1.73	2.54	1955–2015	41	5.89	2.15	4.7	344
6. Hellegatpolder	−2.25	1.81	2.61	1955–2015	52	6.32	2.56	4.95	301

under storm conditions was accurately simulated using the SWAN model (Vuik et al., 2016). In the current study the wave attenuating capacity of foreshores under different conditions was assessed. Daily occurring environmental settings (with and without vegetation) and environmental settings based on design conditions (event with a statistical recurrence time of 1/10,000 year) were used (Fig. 2). Under design conditions, it was assumed that vegetation present at the marsh was bent over or broken and lying flat at the bed (Vuik et al., 2018a, 2018b).

2.2.1. Vegetation characteristics and bottom roughness

The marsh edge position was determined by using a tidal benchmark, since the marsh edge position was recorded for the full period of data. In literature, the seaward marsh edge has often been approximated by using a tidal benchmark (McKee and Patrick, 1988; Bakker et al., 2002; D'Alpaos et al., 2007; Balke et al., 2016). The tidal benchmark mean high water neap (MHWN) has been used previously to define the marsh edge (Doody, 2007), and this benchmark was used to study salt marsh dynamics in the Westerschelde as well (Van der Wal et al., 2008). Therefore, the tidal benchmark MHWN from Van der Wal et al. (2008) was adopted in the present study to define the salt marsh edge (Table 1).

Vegetation characteristics at the marsh edge were obtained by Vuik et al. (2016), for the brackish salt marsh Zimmermanpolder (3; called Bath in Vuik et al. (2016)) and more salty salt marsh Hellegatpolder (6). The brackish species *Scirpus* maritimus was found at Zimmermanpolder (3), while the salty species *Spartina anglica* was found at Hellegatpolder (6). More mixed vegetation was present at the higher marsh, but was not taken into account, because a major part of the waves is attenuated at the marsh edge, especially under daily conditions. Collected vegetation characteristics have been averaged to obtain general values for the mean vegetation height (h_{veg}), stem density ($N_{v,0}$), stem thickness ($b_{v,0}$) and these values were used as input for SWAN (Table 2). The general characteristics derived from both salt marshes were assumed to be representative for the whole Westerschelde.

Under daily conditions, the long-term contribution of vegetation to the wave attenuating capacity of foreshores was assessed by explicitly including and excluding vegetation in wave modelling. The scenario

including vegetation was assumed to be representative for summer conditions with maximum biomass, while the scenario excluding vegetation was assumed to be representative for winter conditions, with minimum vegetation biomass. Daily conditions without vegetation in scenario 1 (panel 1, Fig. 2) were represented with a constant Nikuradse roughness length scale ($k_{N,bare flat}$) of 0.001 m for the entire profile (Vuik et al., 2019), for only assessing the contribution of the morphology. The Nikuradse values used, are derived from Manning roughness coefficients presented in Wamsley et al. (2010), by using the conversion equation in Bretschneider et al. (1986). Vegetation was explicitly included in the model in scenario 2 (panel 2, Fig. 2). Daily conditions with vegetation were represented with a Nikuradse roughness length scale of 0.001 m at the bare tidal flat ($k_{N,bare flat}$) and 0.02 m at the vegetated foreshore ($k_{N, veg. marsh daily}$) representing the bed under the vegetation (Vuik et al., 2016, Table 2). Under design conditions, scenario 3 (panel 3, Fig. 2), the roughness at the marsh due to broken vegetation was represented by a Nikuradse roughness length scale $k_{N,veg. marsh design}$ of 0.05 m (Wamsley et al., 2010), whereas the roughness at the bare tidal flat in front of the marsh ($k_{N,bare flat}$) was represented again with the value of 0.001 m (Vuik et al., 2019). So following Vuik et al. (2019), vegetation in scenario 3 was not included in SWAN using the vegetation module, but using an adapted Nikuradse roughness length.

2.2.2. Hydrodynamic boundary conditions

Hydrodynamic boundary conditions for approximating the daily wave attenuating capacity (panel 1 & 2, Fig. 2) representing the water level were derived from tidal characteristics. Mean High Water Spring (MHWS), being the highest common occurring water level at which large parts of the salt marsh contribute to wave attenuation, was derived from Van der Wal et al. (2008). Daily wave characteristics used, were $H_{m0,daily} = 0.2$ m and $T_{m-1,0,daily} = 3$ s (Callaghan et al., 2010; Hu et al., 2015a, 2015b) (Table 2; Fig. 2). Energy gain due to wind was not accounted for in the calibrated SWAN model (Vuik et al., 2016), since wind input was assumed to be insignificant over small foreshore lengths.

The hydrodynamic boundary conditions under design conditions (panel 3, Fig. 2; Table 1) were obtained from the WTI (legal assessment

Table 2
General input parameters for wave modelling.

| Parameter	Symbol	Value	Unit	Source
Daily wave height	$H_{m0,daily}$	0.2	m	Callaghan et al. (2010); Hu et al. (2015a)
Daily wave period	$T_{m-1,0,daily}$	3	s	Hu et al. (2015b)
Mean vegetation height	h_{veg}	0.24	m	Vuik et al. (2016)
Vegetation stem density	$N_{v,0}$	865	$1/m^2$	Vuik et al. (2016)
Vegetation stem thickness	$B_{v,0}$	5.1	mm	Vuik et al. (2016)
Nikuradse roughness length scale for bare tidal flats	$k_{N,bare flat}$	0.001	m	Vuik et al. (2019)
Nikuradse roughness length scale for salt marsh under design conditions	$k_{N,veg.marsh design}$	0.05	m	Vuik et al. (2019); Wamsley et al. (2010)
Nikuradse roughness length scale for salt marsh under daily conditions	$k_{N,veg. marsh daily}$	0.02	m	Vuik et al. (2016)
Bulk drag coefficient	C_D	1.0	–	Suzuki and Arikawa (2010)
Transect spacing	SpacT	250	m	Transect refinement (section 2.2.3.)

instrument; in Dutch: 'wettelijk toetsingsinstrumentarium') (Gautier and Groeneweg, 2012; Groeneweg and Van Nieuwkoop, 2015) representing an event statistically occurring once every 10,000 year. This safety level has been used previously to assess the safety of the Dutch dikes. Both water levels and wave characteristics are available along every 250 m of coastline. Water levels, wave period and wave height at the eastern and western side of each study site were averaged, thereby avoiding hydrodynamic parameters that were influenced by the topography of the study site (e.g. by refraction and shoaling) (top panel, Fig. 3). The design wave direction was selected at the center of the salt marsh (Table 1). Herein is the wave direction the result of the wind direction and rotation due to refraction.

Bulk drag coefficients C_D were derived in Vuik et al. (2016) by calibrating the SWAN model for optimal reproduction of measured wave attenuation by vegetation. However, these calibrated values were meant to describe wave attenuation during storms, for which flexibility of vegetation plays an important role. This resulted in values significantly below 1.0. The current study explicitly includes vegetation structures for wave attenuation under daily conditions (panel 2, Fig. 2), with small waves and low water depth. In these circumstances, bending of the plants will be limited, and we assumed the drag force will resemble that of rigid cylinders, for which a value of approximately 1.0 is appropriate (Suzuki and Arikawa, 2010). Therefore, $C_D = 1.0$ is taken into account in all SWAN simulations for daily conditions explicitly including vegetation (scenario 2).

2.2.3. Transect refinement

To assess the wave attenuating capacity of a foreshore, the landscape
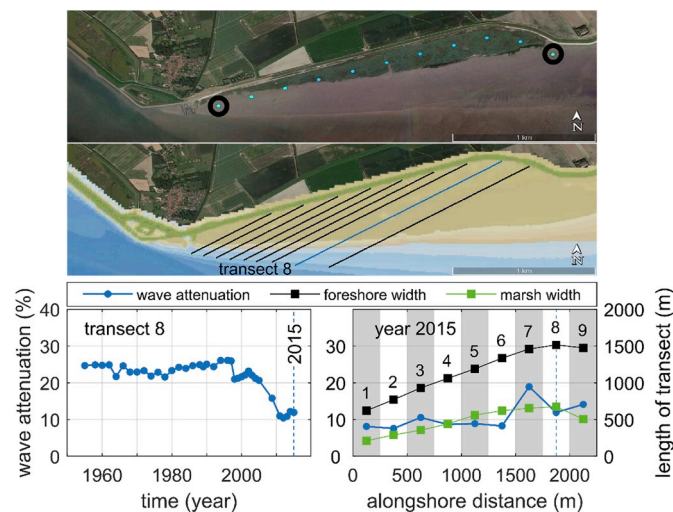
Fig. 3. The method for assessing wave attenuation at the foreshore Zuidgors for a single transect and a single year. The top panel shows locations (blue dots) where significant wave heights under design conditions were provided (Gautier and Groeneweg, 2012; Groeneweg and Van Nieuwkoop, 2015). Hydrodynamic characteristics (water level, wave height, wave direction) at both alongshore boundaries of the foreshores were averaged to obtain boundary conditions for the wave model (black circles; top panel). The bed elevation was derived from the Vaklodingen dataset (background colors in center panel indicate the bathymetry of 2014). Transects parallel to the design wave direction with an alongshore spacing of 250 m, measured at the dike, are indicated with black lines (center panel). The blue line (center panel) highlights transect 8, for which the temporal variation of wave attenuation is shown (bottom left panel). The vertical dashed blue line (bottom left panel) highlights the last year assessed (2015). The wave attenuating capacity in the last year 2015 for all nine transects at the marsh is highlighted with the blue line (left vertical axis; bottom right panel). The black line indicates the width of the assessed foreshore, whereas the green line indicates the width of the vegetated salt marsh (both on the right vertical axis). (For interpretation of the references to color in this figure legend, the reader is referred to the Web version of this article.)

was represented using transects parallel to the design wave direction (center panel, Fig. 3). The spacing between the transects (i.e. the alongshore distance between two transects) was selected in a way that the spatial variability of the foreshores was fully captured. The geometry of the foreshore for a specific transect and associated wave attenuating capacity was calculated for transects with a different alongshore spacing, i.e. the distance between transects was measured over the landward stretch of the dike to be able to relate the results to dike safety. An initial spacing of 1000 m was selected, because the alongshore length of the foreshores just exceeded 1000 m at some foreshores. A transect spacing of 1000 m does not include the minimum and maximum transect width of the foreshore, and as a consequence neither the full variability in wave attenuation. The same holds for a transect spacing of 500 m. The full variability of the foreshore was captured by a transect spacing of 250 m, a smaller spacing of e.g. 125 m did not add more detail. So a transect spacing of 250 m was selected to capture the maximum variability with the largest spacing (i.e. least amount of transects) for computational efficiency (bottom panels, Fig. 3).

3. Results

3.1. Long-term foreshore geometry

3.1.1. Temporal variability

The foreshore geometry was assessed by analyzing historical bed level data. The cross-shore width of both the vegetated salt marsh and complete foreshore (between MLWS and MHWS) were found to be variable over space and time. The width of the vegetated part did not follow the total width of the foreshore per definition. At a representative transect at Paulinapolder, the width of the total foreshore increased by a 100 m over 60 years. Nevertheless the width of the salt marsh was highly variably with a minimum width of 80 m and a maximum width of 310 m in the first decades (Fig. 4 location PAU). Moreover, at Zimmermanpolder the total foreshore width in the first decade was decreasing (from 1530 m to 1140 m), while the width of the vegetated part was increasing with tens of meters (Fig. 4, location ZIM). Zooming in on the single foreshores, the average width (averaged over all transects of the foreshore) of the bare tidal flat was always larger than the average width of
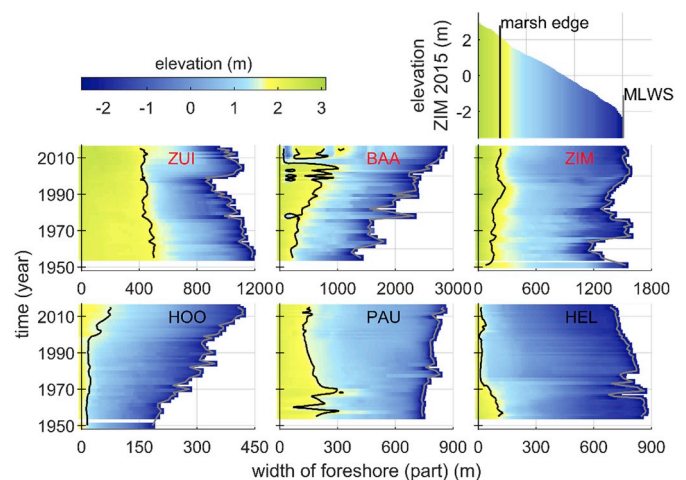
Fig. 4. Change in width of foreshore (horizontal axis) in time (vertical axis) for the 6 foreshores studied. The color indicates the elevation with respect to mean sea level, whereas the black line indicates the marsh edge and the grey line mean low water spring (MLWS). Per foreshore, a representative transect is chosen and followed in time, as shown for Zimmerman in 2015 (top right). Abbreviations indicate locations as indicated in Fig. 1; red letters highlight exposed sites, while black letters highlight sheltered sites from the prevailing wind direction. (For interpretation of the references to color in this figure legend, the reader is referred to the Web version of this article.)
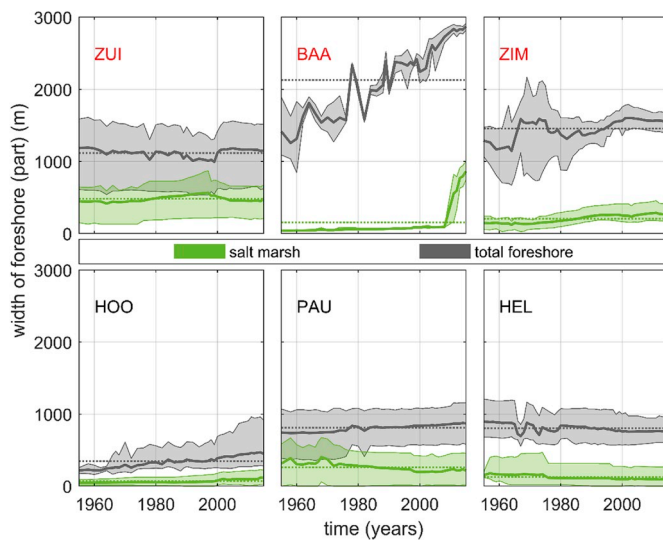
Fig. 5. Change in width of the foreshore (vertical axis) over time (horizontal axis) in which distinction is made in salt marsh width (green area) and total foreshore width (grey area) The shading indicates the minimum and maximum width, the thick line in the center of the shading indicates the spatial mean width and the dotted line indicates the overall mean width. Abbreviations indicate locations as indicated in Fig. 1; red letters highlight exposed sites, while black letters highlight sheltered sites from the prevailing wind direction. (For interpretation of the references to color in this figure legend, the reader is referred to the Web version of this article.)

Fig. 6. Marsh width change (vertical axis) over a period of a single year, periods between 1 and 10, 11 and 20, 21 and 30, 31 and 40 and 50 years (horizontal axis). The white marker indicates the median, the 10th and 90th percentile are highlighted by the black bar, while the whiskers at the top and bottom of the black bar indicate the maximum and minimum change over a specific period. Abbreviations indicate locations as indicated in Fig. 1; red letters highlight exposed sites, while black letters highlight sheltered sites from the prevailing wind direction. (For interpretation of the references to color in this figure legend, the reader is referred to the Web version of this article.)

the adjacent vegetated salt marsh, i.e. on average the part of the foreshore covered by vegetation does never exceed 50% (Fig. 5). The part of the foreshore covered by vegetation was relatively high at Zuidgors and Paulinapolder, exceeding 32%, while below 20% at the other foreshores. In general the mean width of the salt marsh remained stable (except during the last decade at Baarland), whereas the mean width of the total foreshore showed a more dynamic behavior (Fig. 5). At Zuidgors, Baarland, Zimmermanpolder and Hellegatpolder changes of hundreds of meters occurred within a period of 5 years only. The latter is supported by strong changes of the total foreshore width observed at a single representative transect in periods of a few years only, e.g. in the first decades of the analysis at Zimmermanpolder (ZIM) and Hellegatpolder (HEL) and the last decade at Baarland (BAA) (Fig. 4).

The change of the width of the vegetated salt marsh over a period of a single year remained small, with a change of maximum tens of meters in the range of the 10th and 90th percentile (Appendix A). Both positive and negative outliers of hundreds of meters were observed over a single year (Fig. 6; Appendix A). The marsh width change increased with increasing length of observation periods, i.e. the longer the observation period, the larger the difference between maximum and minimum width of the salt marsh width, indicating a continuous change over the entire period. However, when observing the change over the longest periods (marsh width change over more than 30 years), the change in width decreased. Moreover, the range between minimum and maximum change was largest over the periods between 11 and 20 and 21 and 30 years, with differences between the minimum and maximum of 100–200 m at e.g. Hoofdplaat (smallest) and almost a kilometer at Baarland (largest). While the range becomes constant or even decreases over the long-term, the median of the change shows different behavior per entire foreshore. A continuous increase was observed at Baarland (0–60 m), Zimmermanpolder (5–130 m), and Hoofdplaat (0–33 m), while a decreasing marsh width was observed at Paulinapolder (0 to −115 m) and Hellegatpolder (0 to −55 m). At Zuidgors (between -5 m and 25 m) the median change was observed to vary around zero (Appendix A). It was striking that in general, the largest increase in marsh width change (between 10th and 90th percentile) occurred in periods

between 1 and 10 years and 11 and 20 years (Fig. 6). This observation in combination with a flattening range between the maximum and minimum marsh width change over the long-term might indicate an increasing stability over a longer period.

3.1.2. Spatial variability

At Zuidgors, the average width of the salt marsh (483 m; see Appendix A; table 9, for the average width of the vegetated salt marsh and bare tidal flat of all foreshores) was observed to be much smaller than the width of the total foreshore (1116 m) (Fig. 5). However, the width of the vegetated salt marsh in a single year was highly variable, showing differences of up to 600 m over an alongshore salt marsh stretch of 2000m (Fig. 5). The most western part of the foreshore at Zuidgors showed less variability in foreshore width compared to the eastern part, probably due to the geographical features surrounding the foreshore. One of the main features is the presence of a channel in front of the foreshore (Fig. 1; top panels, Fig. 3). The vegetated foreshore part at the eastern side of the center has more landward accommodation space, due to the shape of the dike. Due to the contribution of those boundaries, the spatial variability remained stable (Figs. 4 and 5). Geographical features like dikes and jetties, did also drive the spatial variability within a single year at the other locations. At Baarland, Zimmermanpolder and Paulinapolder, the salt marsh width is smaller at the alongshore edges of marsh, while being larger at the central part of the marsh due to the recessed dike, similar to Zuidgors. At Hoofdplaat and Hellegatpolder jetties and an outflow channel affect the spatial variability of the salt marsh. At Baarland the spatial variability of both the total foreshore and the salt marsh remained small, with some peaks up to a 1000 m for the foreshore and hundreds of meters at the salt marsh. The little variability might be caused by a small channel appearing close to the salt marsh edge (Fig. 1). At Zimmermanpolder the spatial variability of the salt marsh was approximately 200 m, whereas the spatial variability of the total foreshore reached 1200 m. The spatial variability of the foreshores at the sheltered shores remained constant (Fig. 5), being 300–500 m for both the total foreshore and salt marsh at Hellegatpolder and Paulinapolder, while both the average width and variability increased at Hoofdplaat (Fig. 5).

3.1.3. Spatial versus temporal variability

The width of transects between MLWS and MHWS of a single foreshore was highly variable, e.g. at Zuidgors ranging between 600 m and 1500 m (Fig. 3). However, the spatial variability remained constant over time, i.e. the range of the width of all transects of a single foreshore remained stable (Fig. 5). The spatial variability of the salt marsh at Zuidgors slightly decreased with tens of meters only, this was observed more distinct at the sheltered site Hellegatpolder with approximately 200 m, whereas an increasing spatial variability was observed at Hoofdplaat both for the total foreshore and salt marsh. The average total foreshore width increased with 250 m, while the variability increased from less than 100–600 m. Those changes might have been the result of accretion between the jetties and/or changes in the seaward navigation channel. Large differences of spatial variability over time was observed at Zimmermanpolder, in the first decades. Nevertheless the variability of the foreshore in a single year decreased from a maximum of 1200–260 m, while the width of the salt marsh remained constant over time (Fig. 5). Most striking was the temporal variability at Baarland, where the total foreshore width increased from approximately 1400–2800 m and the salt marsh width increased from 40 m to 860 m, while the spatial variability was small.

In general, the average width of foreshore parts of a single foreshore was larger in space than in time, i.e. the width of the foreshore (parts) remained constant over time while more variation was observed over a single foreshore in a single year (Fig. 5). However there were exceptions, the temporal variation at Baarland was larger than the spatial variation, probably due to a small channel in front of the foreshore undershooting MLWS, only appearing in a part of the assessed period. The, in general larger, spatial variability indicated that the alongshore variability of the geometry caused by geographical boundaries (e.g. dikes and channels), was larger than the variability of a single transect influenced by hydrodynamics, morphodynamics and vegetation growth. The latter implies that a large part of the variability of the foreshore geometry captured in a single observation, represents the variability of the width of the foreshore (parts) over the long-term (60–70 years).

3.1.4. Exposed shores versus sheltered shores

The average width of foreshores, parallel to the design wind direction, in the Westerschelde ranged between 344 m and 2130 m (Fig. 5), with an average vegetated part ranging between 7% and 42% of the total foreshore width. The average width of the foreshores at the northern shores (1583 m), exposed to the prevailing wind direction, of the Westerschelde was larger than at the southern shores (652 m), sheltered from the prevailing wind direction. Therefore the foreshores at the sheltered shores consisted of a steeper gradient, since the width was measured between two vertical positions fixed in time (MHWS and MLWS). The average salt marsh width at the exposed shores was 280 m, whereas 151 m at the sheltered shores. This is a vegetated part of 18% and 23% respectively. In general the smaller sheltered foreshores showed a smaller marsh width change over the assessed period. However, it appeared that the marsh at the sheltered foreshores were retreating (PAU and HEL) or slightly increasing (HOO). The marshes at the exposed foreshores were relative stable (ZUI) or even expanding (BAA and ZIM), in spite of their location exposed to the prevailing wind direction (Fig. 6).

3.2. Long-term wave attenuating capacity

The wave attenuation was calculated for three different scenarios, (1) attenuation under daily conditions over the transects, (2) attenuation under daily conditions over the transects, explicitly accounting for vegetation, and (3) attenuation under design conditions over the transects, accounting for broken vegetation (Fig. 2). The wave attenuating capacity of a single transect was defined as the smallest value found for the wave attenuation for the assessed period, to indicate the natural capacity of the foreshore, without additional management. Those values for all transects of a single foreshore, result in a characteristic range of the wave attenuating capacity of a single foreshore. The transect with the smallest wave attenuation marks the lower limit of the range.

3.2.1. Daily conditions

The range of wave attenuation under daily conditions (scenario 1) was large, between 10% and 100% at the exposed shores and 0% and 100% at the sheltered shores. The large wave attenuation was almost entirely the result of attenuation at the salt marsh. Inclusion of vegetation (scenario 2), representing summer conditions, leads to higher wave attenuation and a lower variability, especially at the foreshores located at the exposed shores. The attenuation ranged between 60% and 100%, with only a single lower peak at Zuidgors and Baarland of approximately 30%–40%. Under both scenarios for daily conditions, the waves were almost always fully attenuated by the foreshore, probably due to depth-induced wave breaking. Nevertheless, this was at least partly accomplished by the presence of vegetation, stabilizing the profile. The comparison of the wave attenuation for both scenarios under daily conditions indicates that vegetation increased the wave attenuating capacity of the foreshore and decreased the variability of wave attenuating capacity of the foreshore, thereby decreasing the wave load at the dike.

3.2.2. Design conditions

Under design conditions, a significant contribution to the wave attenuation was observed for all transects (Fig. 7). The largest contribution to wave attenuation under design conditions was observed at foreshores with a wide vegetated part. For foreshores with a relatively small vegetated part, the bare tidal flat was a large contributor to wave attenuation (up to 18%) (Fig. 8). In general, a constant baseline attenuation of 2%–18% was the result of wave attenuation by the tidal flat. Whereas attenuation as a result of the salt marsh was more variable, more or less following the width of the salt marsh. At most foreshores, the spatial variability of the wave attenuation in a single year (spatially; e.g. 5%–20% at Zuidgors), exceeded the temporal variability of a single transect over the entire measurement period. However, this cannot be adopted as a general rule, e.g. at Baarland the temporal variability was larger than the spatial variability. Moreover, in some years the spatial variability of the wave attenuating capacity could have been neglected, while the temporal variability of a single transect over the assessed period was 20% (comparing a vertical spatial and horizontal temporal cross-section in Fig. 7).

A general relation between width of the foreshore and wave attenuation under design conditions was not found. However, when distinguishing the wave attenuation by the vegetated salt marsh and bare tidal flat, a unique relation per foreshore was observed. The wave attenuation of the salt marsh was found to be a function of the width of the salt marsh (Fig. 8). The longer the salt marsh, the larger the wave attenuation under design conditions, given a maximum observed marsh length of approximately 1000 m. A fit of the relation showed a rather strong approximation (R^2: ZUI is 0.61; BAA is 0.99; ZIM is 0.87; HOO is 0.76; PAU is 0.86; HEL is 0.86), with the smallest R^2 at Zuidgors, also indicated by the 95%-confidence interval (Fig. 8; coefficients for the linear model $y = ax + b$ are presented in Appendix B, where y is the wave attenuation, x is the vegetated marsh width and a and b are the linear coefficients). A clear distinction was observed between the foreshores at the exposed and sheltered shores of the Westerschelde. The wave height, water level ratio under extreme conditions was also larger at the sheltered shores, due to slightly lower water levels and larger waves, which might possibly affect the effectiveness of the wave attenuation. The wave attenuation at the sheltered foreshores was larger per meter of salt marsh, despite the shorter width of both the total foreshore and salt marsh. So the effectiveness of wave attenuation under design conditions, per meter marsh width, was observed to be larger for the foreshores with a smaller width.
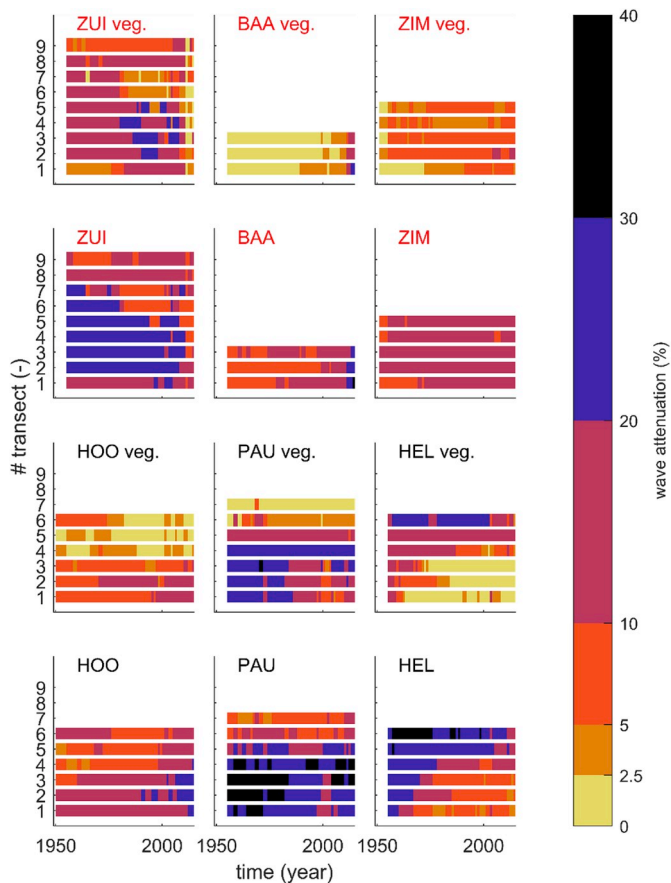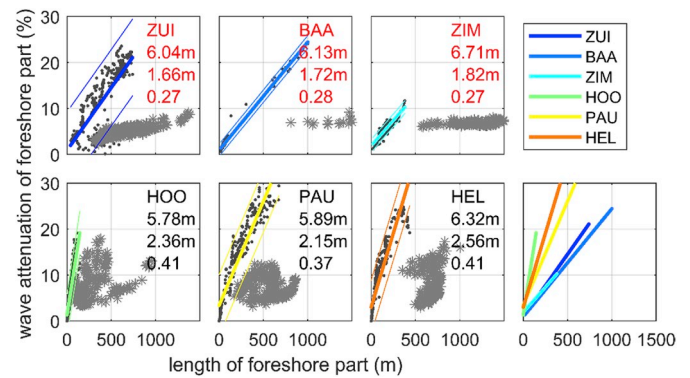
Fig. 7. Wave attenuation (i.e. % of incoming wave; indicated by colors) under design conditions (i.e. extreme event statistically occurring once every 10,000 years) for both the vegetated part of the foreshore (panels with "veg." behind location name) and the total foreshore. The time is indicated at the horizontal axis, whereas the different transects are presented at the vertical axis. Abbreviations indicate locations as indicated in Fig. 1; red letters highlight exposed sites, while black letters highlight sheltered sites from the prevailing wind direction. (For interpretation of the references to color in this figure legend, the reader is referred to the Web version of this article.)

4. Discussion

The decadal persistence of wave-attenuating ecosystems was identified as key-bottle neck hampering application of intertidal foreshores for coastal protection (Bouma et al., 2014). In this study, the decadal wave attenuating capacity of foreshores under daily and extreme conditions was studied estuarine-wide. The key-findings were: (1) foreshores always contribute to wave attenuation both under daily and design conditions; (2) under daily conditions, vegetation contributes to decreasing wave energy and decreases the variability of incoming wave energy; (3) under design conditions, foreshores located at shores sheltered from the prevailing wind direction were more efficient in wave attenuation than foreshores located at exposed shores, which might be related to the geometry of the foreshore. Moreover, the bare tidal flat caused a baseline wave attenuation, while the additional contribution of the vegetated salt marsh appeared to be related to marsh width: the larger the marsh width, the larger the wave attenuation.

### 4.1. Contribution of foreshores to coastal safety

The protective value of (vegetated) foreshores by wave attenuation has been proven in recent years, even under extreme conditions (Barbier et al., 2008; Gedan et al., 2011; Shepard et al., 2011; Moller et al., 2014). However, the protective value depends on the bio-geomorphological

Fig. 8. Contribution of both foreshore parts to wave attenuation under design conditions (i.e. extreme event statistically occurring once every 10,000 years) for all transects and years. The width of the bare (grey asterisk) and vegetated foreshore (black dot) are indicated at the horizontal axis, their contribution to the wave attenuation under design conditions is plotted at the vertical axis. The colored thick line per panel, indicates the fit of the relation between vegetated foreshore width and wave attenuation and the colored thin lines indicate the 95% confidence interval. Abbreviations indicate locations as indicated in Fig. 1; red letters highlight exposed sites, while black letters highlight sheltered sites from the prevailing wind direction. The three numbers in each panel characterize the foreshore, from top to bottom: the extreme water level, extreme wave height and the wave height/water level ratio respectively. All relations are summarized in the bottom right panel. (For interpretation of the references to color in this figure legend, the reader is referred to the Web version of this article.)

settings of the foreshore (Vuik et al., 2018b), which vary over time (Bouma et al., 2014). Based on long-term field data and modelling, this study emphasizes the presence of an added value for coastal safety under all bio-geomorphological settings present in an entire estuary (e.g. 6 foreshores, a total of 36 transects, over 65 years). Whereas previous studies calculate the wave attenuating capacity for a single setting, multiple settings not using long-term field measurements and/or the short-term (e.g. Bouma et al., 2010; Yang et al., 2012; Moller et al., 2014; Vuik et al., 2016). This study quantifies the range of wave attenuating capacity under different scenarios for salt marsh settings measured in the field over the long-term. Moreover a minimum wave attenuating capacity was observed from 6% to 12% at the exposed northern shores and 3%–27% at the sheltered southern shores under design conditions (Table 3; Fig. 8). Even wave attenuation under daily conditions always benefits from the presence of vegetation by increasing the wave attenuating capacity and narrowing the bandwidth of incoming waves (i.e. wave height), decreasing the wave load at the dike continuously over 65 years (Fig. 9).

Only the existence of the vegetated foreshores over a period of 60–70 years, already proves the resilience of those ecosystems to external (anthropogenic) influences. Moreover, the width of the foreshore (parts) specifically assessed in this study remained quite similar over time (Fig. 5). The resulting wave attenuation varied over space (transects) and time (development over the assessed period), but delivers a continuous contribution to the wave attenuation (Fig. 9). Nevertheless, the development of foreshores might be less stable in other estuaries, e. g. rapidly expanding near the mouth of the Yangtze river, China (Yang et al., 2001; Zhang et al., 2004), or retreating foreshores affecting the contribution to wave attenuation. Results of the current study delivers prove and builds upon previous studies emphasizing the instantaneous contribution of foreshores to coastal protection (Turner et al., 2007; Kirwan et al., 2010; Gedan et al., 2011). Insights in short to medium-term (days to several years) vegetation establishment and growth, defining the marsh edge and partly the wave attenuating capacity, have been obtained (Bouma et al., 2016; Willemsen et al., 2018; Poppema et al., 2019). However long-term limits (design period) of vegetation growth defining the local range of the width of the vegetated
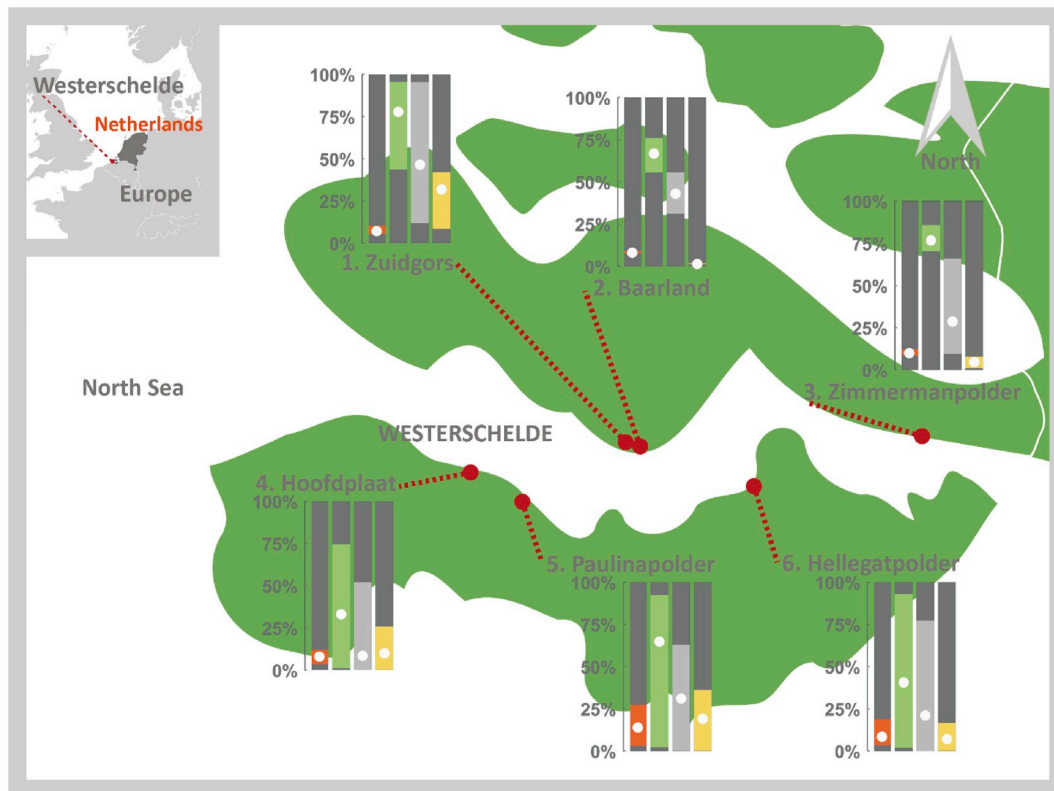
Fig. 9. Summary of the range of wave attenuation averaged per foreshore and the range of width of the vegetated salt marsh. Spatial mean (white dot) and variability (minimum and maximum indicated by the bar) of the wave attenuating capacity under design conditions (orange), daily conditions with explicitly accounting for vegetation (green) and daily conditions without vegetation (grey) and the related coverage of vegetation relative to the total length of the foreshore (yellow). (For interpretation of the references to color in this figure legend, the reader is referred to the Web version of this article.)

foreshore need to be studied, to exploit the relation between the width of the vegetated foreshore and wave attenuation (Fig. 8). This might result eventually in parameter values contributing to stable practical implementation of foreshores as add-on in coastal protection schemes and managing the foreshore to supply, maintain and possibly increase the minimum wave attenuating capacity.

4.2. The location of the marsh edge

This study highlights the importance of the boundary between the bare tidal flat and vegetated salt marsh, since both foreshore parts have a different role in attenuating waves under design conditions. The tidal flat causes a baseline wave attenuation, while unique linear relations were found between the marsh width and the wave attenuation. In this study, the location of the seaward marsh edge was based on tidal characteristics. However, the marsh edge is determined by multiple biophysical processes: it has been hypothesized that the location of the marsh edge is driven by both bed level change and inundation period (Bouma et al., 2016; Willemsen et al., 2018). This might lead to a marsh edge, slightly off MHWN. Moreover, it is assumed that the marsh edge instantly replies to a changing morphology, which is not possible due to a time lag between bio-physical feedback mechanisms (Poppema et al., 2019). However, field measurements on vegetation presence were not available for all the years. So a general tidal characteristic was assumed, similar to previous studies (McKee and Patrick, 1988; Bakker et al., 2002; D'Alpaos et al., 2007; Doody, 2007; Van der Wal et al., 2008). It is expected that this does not or only slightly affect the wave attenuating capacity, since the marsh edge expands or retreats only meters to tens of meters over a period of a single to a few years (Van der Wal et al., 2008). So it might be expected that the relation between vegetation width and wave attenuation becomes even more pronounced when using a more

precise location of the marsh edge.

By comparing wave attenuation between scenario 1 (excluding vegetation) and scenario 2 (explicitly accounting for vegetation), the increasing contribution of vegetation presence was assessed. A clear bandwidth of the wave attenuating capacity was observed with and without vegetation (Fig. 9). Increasing presence of vegetation resulted in an increased maximum wave attenuating capacity at all assessed foreshores. Moreover, at the northern shores the minimum wave attenuating capacity increased as well, thereby decreasing the uncertainty of the wave attenuating capacity due to the presence of vegetation. The latter, probably due to the absence of the very short (vegetated) foreshore parts at the northern shores. The wave attenuating capacity of the short foreshores occurring at the southern shores, might be less dominated by the presence of vegetation.

4.3. Wave attenuating capacity of a foreshore profile

The contribution of the foreshore to water safety is determined by the foreshore bathymetry and (state of the) vegetation (Vuik et al., 2018b). However, both bathymetry and vegetation cover are changing over time and space, due to naturally occurring bio-physical dynamics (Bouma et al., 2014). Bed level change and inundation time determine the cross-shore location of the marsh edge (Bouma et al., 2014; Willemsen et al., 2018), which can change several hundreds of meters over the assessed period of 60–70 years, but only tens of meters over a period of multiple years. The long-term change has been observed to change the wave attenuation of a single foreshore transect.

The cross-shore location of the marsh edge is known to show cyclic alternations between landward retreat and seaward expansion (Allen, 2000; Singh Chauhan, 2009). Consequently, implying that the minimum and maximum wave attenuating capacity might be found by knowing

the extremes of the cyclic behavior. However, cyclic alternations have not been observed in this study. Moreover, all foreshores have location-specific parameters in addition to the width of the vegetated foreshore affecting the wave attenuating capacity. Yet, the width of the salt marsh determines the major part of the wave attenuating capacity and takes into account local settings when zooming in on a single foreshore by the steepness of the relation (Fig. 8).

Differences in wave attenuation of foreshore transects were observed between foreshores located at the exposed northern and sheltered southern shores (Table 3; Fig. 8). The wave attenuating capacity was larger at the exposed shores (Table 3), although the effectivity (i.e. wave attenuation per meter foreshore) was larger at the sheltered shores (Fig. 8). This might be explained by the shape of the foreshore profile, which is shorter and consequently steeper at the southern shores. Moreover, geographic features as (maintained) channels and landward dikes are hard boundaries affecting the shape of the profile. The wave height/water depth - relation under design conditions is larger at the southern shores, locally resulting in a larger impact of the bottom on the wave attenuation, as studied by Maza et al. (2015). Contrasting with the study of Maza et al. (2015), currents were not included, although they might affect wave attenuation over a vegetated area. However, due to the geographical boundaries (e.g. dikes, jetties) in the Westerschelde estuary surrounding the studied foreshores, it was assumed that currents have a minor influence. To our knowledge, experiments including currents with extremes close to parameter values in the current study (water levels up to 6.71 m at the boundary and 4.47 m at the marsh edge and wave heights up to 2.56 m) are not available. Nevertheless, to better understand the long-term wave attenuating capacity of foreshores under extreme conditions it is recommended to study the influence of currents on long-term wave attenuating under extreme conditions at different field sites.

The foreshore is shaped due to exposure to wind direction, with the southern shores more sheltered to the dominant wind direction (Callaghan et al., 2010), although foreshores at the southern shores are exposed to high waves more often (i.e. largest average wave heights) and are exposed to the longest fetches (Van der Wal et al., 2008). So, the steep and short foreshores at the southern shores sheltered from the prevailing wind direction are exposed to the on average largest waves and longest fetches, shaping these foreshores. Regardless the vegetated part of those foreshores are highly effective in attenuating waves, more effective than the northern foreshores exposed to the dominant wind direction with smaller wave heights, wave height/water depth - relation and fetch. This implies the existence of a feedback mechanism between hydrodynamics, foreshore shape and wave attenuation. To better understand the feedback between hydrodynamics (currents and waves), long-term morphology, ecology and wave attenuation on the spatial scale of a landscape, a process-based 2dh or 3d model can provide insights in the dynamics of the foreshore as a whole. Moreover the long-term wave attenuating capacity of the foreshore under a range of hydrodynamic conditions can be studied.

4.4. Implications for global application of nature based flood defenses

Nature Based Flood Defenses (NBFD) are gaining ground globally (Cheong et al., 2013; Temmerman et al., 2013). Although the area of vegetated foreshores declines (e.g. Valiela et al., 2001), the worldwide occurrence of both mangroves and salt marshes is large (Giri et al., 2011; Mcowen et al., 2017). A stable vegetated foreshore contributes to coastal safety under design conditions. By combining an already existing foreshore with a landward dike, or encourage the growth of a vegetated foreshore in front of an already existing dike, existing infrastructure can be more efficiently utilized for coastal protection. By combining previous literature and the knowledge gained in the current study a contribution can be made to the design and maintenance of hybrid coastal defense structures, which is a next step in implementing NBFD. This hybrid coastal protection infrastructure can benefit from the knowledge

gained in this study. The protective value of the already present foreshore or the needed width of the vegetated foreshore under extreme conditions can be estimated, and with that the increase of the dike height that might be prevented. The natural variability of the marsh width over a specific period (Fig. 6), indicates the long-term stability and instantaneous (1 year) changes. When using foreshores as coastal defense, the effect of too large long-term variability on wave attenuation might be counteracted by maintenance. By using the relation of the range of wave attenuation under different scenarios and the foreshore width, quantified in the current study, one might estimate the added value of maintaining a certain foreshore width. However, accommodation space, which should not be accounted for in the minimum wave attenuating capacity of the foreshore, is needed for instantaneous changes driven by e.g. extreme weather events. Maintaining vegetated foreshores to use their wave attenuating capacity, sustains the ecosystem services provided as well. Moreover, by stimulating the growth and expansion of existing, realigned and new vegetated foreshores, ecosystem services such as habitat provision, food production, space for recreation and accessibility over water (e.g. Barbier et al., 2010) might expand as well. Although the precise relation between vegetated foreshore width and wave attenuation under extreme conditions is location-specific, this study already gives insights in the bandwidth of this linear relation and thereby an estimate of the value for coastal protection.

5. Conclusions

Bathymetrical data was analyzed to assess the variability of the geometry of foreshores. This data was combined with bio-physical parameters to calculate the wave attenuation at six study sites in the Westerschelde, the Netherlands, over a period of 60–70 years, which is longer than the lifetime of hard coastal protection structures. Six foreshores were analyzed, three at the northern shores exposed to the prevailing wind direction and three at the southern shores sheltered from the prevailing wind direction of the estuary. A clear distinction was applied to separate the bare tidal flat and vegetated salt marsh, allowing to explicitly study the contribution of the vegetated foreshore (i.e. salt marsh). The foreshores were assessed to unravel the key question of this study: what are the dynamics of foreshores in an estuary over a decadal time-scale and to what extent can foreshores safely act as additional defense measures?

The total foreshore width at the exposed shores appeared to be longer than at the sheltered shores, resulting in steeper profiles at the sheltered shores. In general, the mean value and the temporal variability of the foreshore width and marsh width remained relatively constant over time. Although the foreshore width remained relatively constant, the width of the salt marsh did not follow the dynamics of the total width of the foreshore at the individual transects. In general, the temporal variability of the salt marsh width increased in the first decades, but flattens subsequently, indicating a constant variability of the width over the long-term. The spatial variability of the foreshore geometry was observed to be larger than the temporal variability, implying that a large part of the variability captured in a single observation in time, might represent the variability of the width of the foreshore (parts) over the long-term (60–70 years).

The vegetation present at the foreshore decreased the variability of the wave attenuation under daily conditions, thereby increasing the reliability of the contribution of the foreshore to coastal safety. A continuous contribution to the coastal safety was found under design conditions, decreasing the wave load at the landward dike. A clear distinction was observed between the foreshores at the exposed northern and sheltered southern shores of the Westerschelde. The wave attenuation at the sheltered shores was larger per meter of salt marsh, despite the shorter width of both the total foreshore and salt marsh. So the long-term effectiveness of wave attenuation under design conditions (i.e. wave attenuation per meter of vegetated salt marsh) was observed to be

larger for the foreshores with a smaller width and steeper profile. In general, the tidal flat caused a baseline wave attenuation under all circumstances, while a linear relation was found between the wave attenuation and the width of the salt marsh, given a maximum observed marsh length of approximately 1000 m. The longer the vegetated salt marsh, the larger the wave attenuation. The relations found, valid for an entire foreshore, can contribute to designing hybrid structures for coastal defense.

CRediT authorship contribution statement

Pim W.J.M. Willemsen: Conceptualization, Methodology, Software, Formal analysis, Investigation, Data curation, Writing - original draft, Writing - review & editing, Visualization, Project administration. **Bas W. Borsje:** Conceptualization, Writing - review & editing, Visualization, Supervision, Funding acquisition. **Vincent Vuik:** Methodology, Software, Validation, Writing - review & editing. **Tjeerd J. Bouma:** Data curation, Writing - review & editing, Supervision, Funding acquisition. **Suzanne J.M.H. Hulscher:** Resources, Writing - review & editing, Supervision, Funding acquisition.

Appendix A

Table 3
Marsh width change over a period of a single year, periods between 1 and 10, 11 and 20, 21 and 30, 31 and 40 and 50 years, for Zuidgors.

Zuidgors (ZUI)	Median (m)	Minimum (m)	Maximum (m)	10th percentile (m)	90th percentile (m)
1 year	0	−160	120	−30	15
1–10 years	0	−210	280	−65	40
11–20 years	−5	−225	310	−105	100
21–30 years	10	−165	365	−100	175
31–40 years	25	−135	350	−84	235
41–50 years	15	−160	375	−100	230

Table 4
Marsh width change over a period of a single year, periods between 1 and 10, 11 and 20, 21 and 30, 31 and 40 and 50 years, for Baarland.

Baarland (BAA)	Median (m)	Minimum (m)	Maximum (m)	10th percentile (m)	90th percentile (m)
1 year	0	−35	295	−5	95
1–10 years	5	−35	915	−5	194
11–20 years	50	−20	930	5	715
21–30 years	30	−15	945	15	725
31–40 years	40	10	955	20	740
41–50 years	60	20	965	40	800

Table 5
Marsh width change over a period of a single year, periods between 1 and 10, 11 and 20, 21 and 30, 31 and 40 and 50 years, for Zimmermanpolder.

Zimmermanpolder (ZIM)	Median (m)	Minimum (m)	Maximum (m)	10th percentile (m)	90th percentile (m)
1 year	5	−55	45	−5	10
1–10 years	10	−75	105	−15	50
11–20 years	45	−65	195	−5	105
21–30 years	75	−25	225	30	160
31–40 years	105	30	265	55	185
41–50 years	130	30	285	65	210

Table 6
Marsh width change over a period of a single year, periods between 1 and 10, 11 and 20, 21 and 30, 31 and 40 and 50 years, for Hoofdplaat.

Hoofdplaat (HOO)	Median (m)	Minimum (m)	Maximum (m)	10th percentile (m)	90th percentile (m)
1 year	0	−25	50	−5	15
1–10 years	5	−45	90	−5	35
11–20 years	20	−40	115	−15	65
21–30 years	20	−45	125	−15	80
31–40 years	20	−50	125	−20	90
41–50 years	33	−50	130	−25	110

Table 7
Marsh width change over a period of a single year, periods between 1 and 10, 11 and 20, 21 and 30, 31 and 40 and 50 years, for Paulinapolder.

Paulinapolder (PAU)	Median (m)	Minimum (m)	Maximum (m)	10th percentile (m)	90th percentile (m)
1 year	0	−100	130	−15	25
1–10 years	0	−215	215	−80	45
11–20 years	−10	−285	170	−135	25
21–30 years	−55	−305	45	−200	10
31–40 years	−95	−325	20	−255	10
41–50 years	−115	−340	20	−260	10

Table 8
Marsh width change over a period of a single year, periods between 1 and 10, 11 and 20, 21 and 30, 31 and 40 and 50 years, for Hellegatpolder.

Hellegatpolder (HEL)	Median (m)	Minimum (m)	Maximum (m)	10th percentile (m)	90th percentile (m)
1 year	0	−35	65	−10	5
1–10 years	0	−155	215	−35	15
11–20 years	−10	−160	270	−85	10
21–30 years	−35	−215	115	−95	10
31–40 years	−45	−205	115	−125	0
41–50 years	−55	−205	110	−140	15

Table 9
Average width (m) of the marsh and bare tidal flat over the assessed period and all transects per foreshore.

Location	Average width marsh (m)	Average width bare tidal flat (m)
Zuidgors (ZUI)	483	634
Baarland (BAA)	152	1977
Zimmermanpolder (ZIM)	205	1253
Hoofdplaat (HOO)	69	275
Paulinapolder (PAU)	258	552
Hellegatpolder (HEL)	125	677

Appendix B

Table 10
Coefficients for determining relation between the vegetated marsh width and wave attenuation. The relation can be determined using $y = ax + b$, where a and b are linear coefficients, y is the wave attenuation and x is the width of the marsh.

Location	Coefficient a	Coefficient b
Zuidgors (ZUI)	0.0273	0.8726
Baarland (BAA)	0.0235	0.9051
Zimmermanpolder (ZIM)	0.0222	1.8731
Hoofdplaat (HOO)	0.1232	1.3113
Paulinapolder (PAU)	0.0453	3.3875
Hellegatpolder (HEL)	0.0643	3.0042

References

Bouma, T.J., van Belzen, J., Balke, T., Zhu, Z., Airoldi, L., Blight, A.J., et al., 2014. Identifying knowledge gaps hampering application of intertidal habitats in coastal protection: opportunities & steps to take. Coast Eng. 87, 147–157. https://doi.org/10.1016/j.coastaleng.2013.11.014.

Marijs, K., Parée, E., 2004. Nauwkeurigheid vaklodingen Westerschelde en monding: "de praktijk.

Poppema, D.W., Willemsen, P.W.J.M., de Vries, M.B., Zhu, Z., Borsje, B.W., Hulscher, S.J.M.H., 2019. Experiment-supported modelling of salt marsh establishment. Ocean Coast Manag. 168, 238–250. https://doi.org/10.1016/j.ocecoaman.2018.10.039.

Allen, J.R.L., 2000. Morphodynamics of Holocene salt marshes: a review sketch from the Atlantic and southern North sea coasts of Europe. Quat. Sci. Rev. 19 (12), 1155–1231. https://doi.org/10.1016/S0277-3791(99)00034-7.

Andersen, T.J., Pejrup, M., Nielsen, A.A., 2006. Long-term and high-resolution measurements of bed level changes in a temperate, microtidal coastal lagoon. Mar. Geol. 226 (1), 115–125. https://doi.org/10.1016/j.margeo.2005.09.016.

Bakker, J.P., Esselink, P., Dijkema, K.S., van Duin, W.E., de Jong, D.J., 2002. Restoration of salt marshes in The Netherlands. Hydrobiologia 478 (1), 29–51. https://doi.org/10.1023/a:1021066311728.

Balke, T., Stock, M., Jensen, K., Bouma, T.J., Kleyer, M., 2016. A global analysis of the seaward salt marsh extent: the importance of tidal range. Water Resour. Res. 52 (5), 3775–3786. https://doi.org/10.1002/2015WR018318.

Barbier, E.B., Koch, E.W., Silliman, B.R., Hacker, S.D., Wolanski, E., Primavera, J., et al., 2008. Coastal ecosystem-based management with nonlinear ecological functions and values. Science 319 (5861), 321–323.

Barbier, E.B., Hacker, S.D., Kennedy, C., Koch, E.W., Stier, A.C., Silliman, B.R., 2010. The value of estuarine and coastal ecosystem services. Ecol. Monogr. 81 (2), 169–193. https://doi.org/10.1890/10-1510.1.

Booij, N., Ris, R.C., Holthuijsen, L.H., 1999. A third-generation wave model for coastal regions: 1. Model description and validation. J. Geophys. Res.: Oceans 104 (C4), 7649–7666. https://doi.org/10.1029/98JC02622.

Borsje, B.W., van Wesenbeeck, B.K., Dekker, F., Paalvast, P., Bouma, T.J., van Katwijk, M.M., de Vries, M.B., 2011. How ecological engineering can serve in coastal protection. Ecol. Eng. 37 (2), 113–122. https://doi.org/10.1016/j.ecoleng.2010.11.027.

Bouma, T.J., De Vries, M.B., Low, E., Peralta, G., Tánczos, I.C., van de Koppel, J., Herman, P.M.J., 2005. TRADE-OFFS related to ecosystem engineering: a case study ON stiffness OF emerging macrophytes. Ecology 86 (8), 2187–2199. https://doi.org/10.1890/04-1588.

Bouma, T.J., van Duren, L.A., Temmerman, S., Claverie, T., Blanco-Garcia, A., Ysebaert, T., Herman, P.M.J., 2007. Spatial flow and sedimentation patterns within patches of epibenthic structures: combining field, flume and modelling experiments. Cont. Shelf Res. 27 (8), 1020–1045. https://doi.org/10.1016/j.csr.2005.12.019.

Bouma, T.J., Vries, M.B.D., Herman, P.M.J., 2010. Comparing ecosystem engineering efficiency of two plant species with contrasting growth strategies. Ecology 91 (9), 2696–2704. https://doi.org/10.1890/09-0690.1.

Bouma, T.J., van Belzen, J., Balke, T., van Dalen, J., Klaassen, P., Hartog, A.M., Herman, P.M.J., 2016. Short-term mudflat dynamics drive long-term cyclic salt marsh dynamics. Limnol. Oceanogr. 61 (6), 2261–2275. https://doi.org/10.1002/lno.10374.

Bretschneider, C., Krock, H., Nakazaki, E., Casciano, F., 1986. Roughness of typical Hawaiian terrain for tsunami run-up calculations: a users manual. JKK Look Lab. Rep. Univ. of Hawaii, Honolulu Hawaii. Report No. 1.

Broekx, S., Smets, S., Liekens, I., Bulckaen, D., De Nocker, L., 2011. Designing a long-term flood risk management plan for the Scheldt estuary using a risk-based approach. Nat. Hazards 57 (2), 245–266. https://doi.org/10.1007/s11069-010-9610-x.

Callaghan, D.P., Bouma, T.J., Klaassen, P., van der Wal, D., Stive, M.J.F., Herman, P.M.J., 2010. Hydrodynamic forcing on salt-marsh development: distinguishing the relative importance of waves and tidal flows. Estuar. Coast Shelf Sci. 89 (1), 73–88. https://doi.org/10.1016/j.ecss.2010.05.013.

Cheong, S.-M., Silliman, B., Wong, P.P., van Wesenbeeck, B., Kim, C.-K., Guannel, G., 2013. Coastal adaptation with ecological engineering. Nat. Clim. Chang. 3 (9), 787–791. https://doi.org/10.1038/nclimate1854.

Coops, H., Geilen, N., Verheij, H.J., Boeters, R., van der Velde, G., 1996. Interactions between waves, bank erosion and emergent vegetation: an experimental study in a wave tank. Aquat. Bot. 53 (3), 187–198. https://doi.org/10.1016/0304-3770(96)01027-3.

D'Alpaos, A., Lanzoni, S., Marani, M., Rinaldo, A., 2007. Landscape evolution in tidal embayments: modeling the interplay of erosion, sedimentation, and vegetation dynamics. J. Geophys. Res.: Earth Surf. 112 (F1) https://doi.org/10.1029/2006JF000537.

De Kruif, A., 2001. Bodemdieptegegevens van het Nederlandse Kustsysteem. Beschikbare digitale data en een overzicht van aanvullende analoge data.

Donnelly, J.P., Cleary, P., Newby, P., Ettinger, R., 2004. Coupling instrumental and geological records of sea-level change: evidence from southern New England of an increase in the rate of sea-level rise in the late 19th century. Geophys. Res. Lett. 31 (5) n/a-n/a.10.1029/2003GL018933.

Doody, J.P., 2007. Saltmarsh Conservation, Management and Restoration, vol. 12. Springer Science & Business Media.

Gautier, C., Groeneweg, J., 2012. Achtergrondrapportage hydraulische belasting voor zee en estuaria.

Gedan, K.B., Kirwan, M.L., Wolanski, E., Barbier, E.B., Silliman, B.R., 2011. The present and future role of coastal wetland vegetation in protecting shorelines: answering recent challenges to the paradigm. Clim. Change 106 (1), 7–29. https://doi.org/10.1007/s10584-010-0003-7.

Gersonius, B., Ashley, R., Pathirana, A., Zevenbergen, C., 2013. Climate change uncertainty: building flexibility into water and flood risk infrastructure. Clim. Change 116 (2), 411–423. https://doi.org/10.1007/s10584-012-0494-5.

Giri, C., Ochieng, E., Tieszen, L.L., Zhu, Z., Singh, A., Loveland, T., et al., 2011. Status and distribution of mangrove forests of the world using earth observation satellite data. Glob. Ecol. Biogeogr. 20 (1), 154–159. https://doi.org/10.1111/j.1466-8238.2010.00584.x.

Groeneweg, J., Van Nieuwkoop, J., 2015. SWAN's Underestimation of Long Wave Penetration into Coastal Systems.

Horstman, E.M., Dohmen-Janssen, C.M., Narra, P.M.F., van den Berg, N.J.F., Siemerink, M., Hulscher, S.J.M.H., 2014. Wave attenuation in mangroves: a quantitative approach to field observations. Coast Eng. 94, 47–62. https://doi.org/10.1016/j.coastaleng.2014.08.005.

Hu, Z., Lenting, W., van der Wal, D., Bouma, T.J., 2015. Continuous monitoring bed-level dynamics on an intertidal flat: introducing novel, stand-alone high-resolution SED-sensors. Geomorphology 245, 223–230. https://doi.org/10.1016/j.geomorph.2015.05.027.

Hu, Z., van Belzen, J., van der Wal, D., Balke, T., Wang, Z.B., Stive, M., Bouma, T.J., 2015. Windows of opportunity for salt marsh vegetation establishment on bare tidal flats: the importance of temporal and spatial variability in hydrodynamic forcing. J. Geophys. Res.: Biogeosciences 120 (7), 1450–1469. https://doi.org/10.1002/2014JG002870.

IPCC, 2014. Climate Change 2014: Synthesis Report. Contribution of Working Groups I, II and III to the Fifth Assessment Report of the Intergovernmental Panel on Climate Change.

Kirwan, M.L., Megonigal, P., 2013. Tidal wetland stability in the face of human impacts and sea-level rise. Nature 504, 53–60. https://doi.org/10.1038/nature12856.

Kirwan, M.L., Guntenspergen, G.R., D'Alpaos, A., Morris, J.T., Mudd, S.M., Temmerman, S., 2010. Limits on the adaptability of coastal marshes to rising sea level. Geophys. Res. Lett. 37 (23) https://doi.org/10.1029/2010GL045489.

Kirwan, M.L., Temmerman, S., Skeehan, E.E., Guntenspergen, G.R., Fagherazzi, S., 2016. Overestimation of marsh vulnerability to sea level rise. Nat. Clim. Chang. 6 (3), 253–260. https://doi.org/10.1038/nclimate2909.

Knutson, T.R., McBride, J.L., Chan, J., Emanuel, K., Holland, G., Landsea, C., et al., 2010. Tropical cyclones and climate change. Nat. Geosci. 3 (3), 157–163. https://doi.org/10.1038/ngeo779.

Lin, N., Emanuel, K., Oppenheimer, M., Vanmarcke, E., 2012. Physically based assessment of hurricane surge threat under climate change. Nat. Clim. Chang. 2, 462. https://doi.org/10.1038/nclimate1389. https://www.nature.com/articles/nclimate1389#supplementary-information.

Maza, M., Lara, J.L., Losada, I.J., Ondiviela, B., Trinogga, J., Bouma, T.J., 2015. Large-scale 3-D experiments of wave and current interaction with real vegetation. Part 2: experimental analysis. Coast Eng. 106, 73–86. https://doi.org/10.1016/j.coastaleng.2015.09.010.

McKee, K.L., Patrick, W.H., 1988. The relationship of smooth cordgrass (Spartina alterniflora) to tidal datums: a review. Estuaries 11 (3), 143–151. https://doi.org/10.2307/1351966.

Mcowen, C.J., Weatherdon, L.V., Bochove, J.-W.V., Sullivan, E., Blyth, S., Zockler, C., et al., 2017. A global map of saltmarshes. Biodivers. Data J. 5 https://doi.org/10.3897/BDJ.5.e11764.

Mendez, F.J., Losada, I.J., 2004. An empirical model to estimate the propagation of random breaking and nonbreaking waves over vegetation fields. Coast Eng. 51 (2), 103–118. https://doi.org/10.1016/j.coastaleng.2003.11.003.

Möller, I., 2006. Quantifying saltmarsh vegetation and its effect on wave height dissipation: results from a UK East coast saltmarsh. Estuar. Coast Shelf Sci. 69 (3), 337–351. https://doi.org/10.1016/j.ecss.2006.05.003.

Moller, I., Kudella, M., Rupprecht, F., Spencer, T., Paul, M., van Wesenbeeck, B.K., et al., 2014. Wave attenuation over coastal salt marshes under storm surge conditions. Nat. Geosci. 7 (10), 727–731. https://doi.org/10.1038/ngeo2251. http://www.nature.com/ngeo/journal/v7/n10/abs/ngeo2251.html#supplementary-information.

Ris, R.C., Holthuijsen, L.H., Booij, N., 1999. A third-generation wave model for coastal regions: 2. Verification. J. Geophys. Res.: Oceans 104 (C4), 7667–7681. https://doi.org/10.1029/1998JC900123.

Shepard, C.C., Crain, C.M., Beck, M.W., 2011. The protective role of coastal marshes: a systematic review and meta-analysis. PLoS One 6 (11), e27374. https://doi.org/10.1371/journal.pone.0027374.

Singh Chauhan, P.P., 2009. Autocyclic erosion in tidal marshes. Geomorphology 110 (3), 45–57. https://doi.org/10.1016/j.geomorph.2009.03.016.

Small, C., Nicholls, R.J., 2003. A global analysis of human settlement in coastal zones. J. Coast. Res. 584–599.

Suzuki, T., Arikawa, T., 2010. Numerical Analysis of Bulk Drag Coefficient in Dense Vegetation by Immersed Boundary Method, vol. 1.

Suzuki, T., Zijlema, M., Burger, B., Meijer, M.C., Narayan, S., 2012. Wave dissipation by vegetation with layer schematization in SWAN. Coast Eng. 59 (1), 64–71. https://doi.org/10.1016/j.coastaleng.2011.07.006.

Syvitski, J.P.M., Kettner, A.J., Overeem, I., Hutton, E.W.H., Hannon, M.T., Brakenridge, G.R., et al., 2009. Sinking deltas due to human activities. Nat. Geosci. 2 (10), 681–686. http://www.nature.com/ngeo/journal/v2/n10/suppinfo/ngeo629_S1.html.

Taal, M., Meersschaut, Y., Liek, G.J., 2015. Understanding the tides crucial for joint management of the Scheldt Estuary. In: Paper Presented at the IAHR World Congres, the Hague, The Netherlands.

Temmerman, S., Meire, P., Bouma, T.J., Herman, P.M.J., Ysebaert, T., De Vriend, H.J., 2013. Ecosystem-based coastal defence in the face of global change. Nature 504 (7478), 79–83. https://doi.org/10.1038/nature12859.

Turner, R.K., Burgess, D., Hadley, D., Coombes, E., Jackson, N., 2007. A cost–benefit appraisal of coastal managed realignment policy. Glob. Environ. Chang. 17 (3), 397–407. https://doi.org/10.1016/j.gloenvcha.2007.05.006.

Valiela, I., Bowen, J.L., York, J.K., 2001. Mangrove forests: one of the world's threatened major tropical environments. Bioscience 51 (10), 807–815. https://doi.org/10.1641/0006-3568(2001)051[0807:mfootw]2.0.co;2.

Van der Wal, D., Wielemaker-Van den Dool, A., Herman, P.M.J., 2008. Spatial patterns, rates and mechanisms of saltmarsh cycles (Westerschelde, The Netherlands). Estuarine. Coast. Shelf Sci. 76 (2), 357–368. https://doi.org/10.1016/j.ecss.2007.07.017.

Van Wesenbeeck, B.K., Van De Koppel, J., Herman, P.M.J., Bouma, T.J., 2008. Does scale-dependent feedback explain spatial complexity in salt-marsh ecosystems? Oikos 117 (1), 152–159. https://doi.org/10.1111/j.2007.0030-1299.16245.x.

Vuik, V., Jonkman, S.N., Borsje, B.W., Suzuki, T., 2016. Nature-based flood protection: the efficiency of vegetated foreshores for reducing wave loads on coastal dikes. Coast Eng. 116, 42–56. https://doi.org/10.1016/j.coastaleng.2016.06.001.

Vuik, V., Suh Heo, H.Y., Zhu, Z., Borsje, B.W., Jonkman, S.N., 2018. Stem breakage of salt marsh vegetation under wave forcing: a field and model study. Estuar. Coast. Shelf Sci. 200, 41–58. https://doi.org/10.1016/j.ecss.2017.09.028.

Vuik, V., van Vuren, S., Borsje, B.W., van Wesenbeeck, B.K., Jonkman, S.N., 2018. Assessing safety of nature-based flood defenses: dealing with extremes and uncertainties. Coast Eng. 139, 47–64. https://doi.org/10.1016/j.coastaleng.2018.05.002.

Vuik, V., Borsje, B.W., Willemsen, P.W.J.M., Jonkman, S.N., 2019. Salt marshes for flood risk reduction: quantifying long-term effectiveness and life-cycle costs. Ocean Coast Manag. 171, 96–110. https://doi.org/10.1016/j.ocecoaman.2019.01.010.

Wamsley, T.V., Cialone, M.A., Smith, J.M., Atkinson, J.H., Rosati, J.D., 2010. The potential of wetlands in reducing storm surge. Ocean Eng. 37 (1), 59–68. https://doi.org/10.1016/j.oceaneng.2009.07.018.

Wiegman, N., Perluka, R., Oude Elberink, S., Vogelzang, J., 2005. Vaklodingen: de inwintechnieken en hun combinaties. Vergelijking tussen verschillende inwintechnieken en de combinaties ervan.

Willemsen, P.W.J.M., Borsje, B.W., Hulscher, S.J.M.H., Van der Wal, D., Zhu, Z., Oteman, B., et al., 2018. Quantifying bed level change at the transition of tidal flat and salt marsh: can we understand the lateral location of the marsh edge? J. Geophys. Res.: Earth Surf. 123 (10), 2509–2524. https://doi.org/10.1029/2018JF004742.

Yang, S.-l., Ding, P.-x., Chen, S.-l., 2001. Changes in progradation rate of the tidal flats at the mouth of the Changjiang (Yangtze) River, China. Geomorphology 38 (1), 167–180. https://doi.org/10.1016/S0169-555X(00)00079-9.

Yang, S.L., Shi, B.W., Bouma, T.J., Ysebaert, T., Luo, X.X., 2012. Wave attenuation at a salt marsh margin: a case study of an exposed coast on the Yangtze estuary. Estuar. Coasts 35 (1), 169–182. https://doi.org/10.1007/s12237-011-9424-4.

Zhang, R.S., Shen, Y.M., Lu, L.Y., Yan, S.G., Wang, Y.H., Li, J.L., Zhang, Z.L., 2004. Formation of Spartina alterniflora salt marshes on the coast of Jiangsu Province, China. Ecol. Eng. 23 (2), 95–105. https://doi.org/10.1016/j.ecoleng.2004.07.007.